The Journal of Nutrition
Nutrient Physiology, Metabolism, and Nutrient-Nutrient Interactions

Glycine Attenuates LPS-Induced Apoptosis and Inflammatory Cell Infiltration in Mouse Liver

Yunchang Zhang,[1] Hai Jia,[1] Yuhang Jin,[1] Ning Liu,[1] Jingqing Chen,[1] Ying Yang,[1] Zhaolai Dai,[1] Chao Wang,[2] Guoyao Wu,[1,3] and Zhenlong Wu[1,4]

[1]State Key Laboratory of Animal Nutrition, Department of Animal Nutrition and Feed Science, China Agricultural University, Beijing 100193, China; [2]State Key Laboratory of Agrobiotechnology, College of Biological Sciences, China Agricultural University, Beijing 100193, China; [3]Department of Animal Science, Texas A&M University, College Station, TX 77843, USA; and [4]Beijing Advanced Innovation Center for Food Nutrition and Human Health, China Agricultural University, Beijing 100193, China

ABSTRACT

Background: Liver dysfunction impairs immunological homeostasis. Glycine (Gly) has been reported to have antioxidative and anti-inflammatory effects and to regulate apoptosis in various models.

Objectives: The aim of the present study was to determine whether Gly could attenuate LPS-induced liver injury.

Methods: In Experiment 1, 48 6-week-old male C57BL/6 mice were randomly assigned into one of 4 groups: CON (control), GLY [orally administered Gly, 5 g · kg body weight $(BW)^{-1}$ · d^{-1} for 6 d], LPS (5 mg/kg BW, intraperitoneally administered), and GLY + LPS (Gly supplementation, and on day 7 LPS treatment). In Experiment 2, mice were untreated, pretreated with Gly as above, or pretreated with Gly + L-buthionine sulfoximine (BSO) (0.5 g/kg BW, intraperitoneally administered every other day) for 6 d. On day 7, mice were injected with LPS as above. Histological alterations, activities of antioxidative enzymes, apoptosis, and immune cell infiltration were analyzed.

Results: In Experiment 1, compared with CON, LPS administration resulted in increased karyolysis and karyopyknosis in the liver by 8- to 10-fold, enhanced serum activities of alanine transaminase (ALT), aspartate transaminase (AST), and lactate dehydrogenase (LDH) by 1- to 1.8-fold, and increased hepatic apoptosis by 5.5-fold. Furthermore, LPS exposure resulted in increased infiltration of macrophages and neutrophils in the liver by 3.2- to 7.5-fold, elevated hepatic concentrations of malondialdehyde and hydrogen peroxide (H_2O_2), and elevated myeloperoxidase (MPO) activity by 1.5- to 6.3-fold. In Experiment 2, compared with the LPS group, mice in the GLY + LPS group had fewer histological alterations (68.5%–75.9%); lower serum ALT, AST, and LDH activities (24.3%–64.7%); and lower hepatic malondialdehyde and H_2O_2 concentrations (46.1%–80.2%), lower MPO activity (39.2%), immune cell infiltration (52.3%–85.3%), and apoptosis (69.6%), which were abrogated by BSO. Compared with the GLY + LPS group, mice in the GLY + BSO + LPS group had lower hepatic activities of catalase, superoxide dismutase, and glutathione peroxidase by 33.5%–48.5%; increased activation of NF-κB by 2.3-fold; and impaired nuclear factor (erythroid-derived 2)-like 2 signaling by 38.9%.

Conclusions: Gly is a functional amino acid with an ability to protect the liver against LPS-induced injury in mice. *J Nutr* 2020;150:1116–1125.

Keywords: apoptosis, glycine, inflammation, lipopolysaccharide, oxidative stress

Introduction

The liver plays a key role in immunological homeostasis and metabolism of both humans and animals (1). Various factors, such as stress insults, alcohol abuse, drug exposure, and bacterial infection, have been reported to contribute to liver dysfunction. LPS, a major endotoxin in gram-negative bacteria, activates the host inflammatory response, leading to the production of cytokines and oxidative stress, which, in turn, damages the liver as characterized by hepatic dysfunction, coagulation disorder, and even liver failure (2).

An essential function of liver is to maintain the intracellular balance between free radicals and antioxidants. Mammals have both enzymatic and nonenzymatic antioxidant systems to regulate the homeostasis of organs in response to cellular oxidative stress (3, 4). Under physiological conditions, the mitochondria-derived reactive oxygen species (ROS) are removed by the antioxidant systems. However, following an exposure to LPS or toxins, an increase in the production of free radicals, such as ROS and reactive nitrogen species, or a decrease in the capacity of antioxidant systems leads to elevated amounts of oxygen radicals. These molecules bind

Manuscript received June 27, 2019. Initial review completed August 30, 2019. Revision accepted February 4, 2020.
First published online February 26, 2020; doi: https://doi.org/10.1093/jn/nxaa036.

to and impair macrobiomolecules (lipid, protein, and DNA), thereby impairing liver function and causing liver diseases (5). Biochemically, LPS activates the NF-κB signaling cascade, which promotes the biosynthesis of proinflammatory cytokines, including TNFa, IL1b, IL6, and chemokines in epithelial cells and immune cells (6). Both inflammatory cytokines and free oxygen radicals have been reported to induce cell death in a caspase-3 dependent manner in response to LPS exposure (7, 8). Therefore, strategies to block the release of inflammatory cytokines and related apoptosis have been investigated in both *in vivo* and *in vitro* models.

Glycine (Gly) has long been classified as a nutritionally nonessential amino acid in mammals and other animals (9). It has been shown to have anti-inflammatory and immunomodulatory effects in the organisms and various cell types (10, 11). In addition, Gly is a substrate for the synthesis of glutathione (GSH), a major endogenous antioxidant required for the maintenance of intracellular homeostasis (12). In our previous studies, we found that Gly was critical for intestinal mucosal barrier function by enhancing protein synthesis (13), regulating the abundance of tight junction proteins (14), and protecting intestinal porcine epithelial cells from 4-hydroxynonenal-induced apoptosis (15). However, the underlying mechanisms responsible for the beneficial effects remain unknown. We hypothesized that Gly can regulate anti-inflammatory response, intracellular ROS homeostasis, and apoptosis, thereby protecting the liver from oxidative stress-induced damage. This hypothesis was tested in the LPS-challenged mouse, a well-known animal model for studies on liver injury and the underlying molecular mechanisms. L-buthionine sulfoximine (BSO), a specific inhibitor of γ-glutamylcysteine synthetase (16), was used in the present study to investigate the functional role of Gly-driven GSH synthesis on LPS-induced liver injury.

Methods

Reagents

LPS (*Escherichia coli*, 055: B5) and Gly were products of Sigma. BSO was purchased from Santa Cruz Biotechnology. Alanine transaminase (ALT), aspartate transaminase (AST), lactate dehydrogenase (LDH), superoxide dismutase (SOD), catalase (CAT), glutathione peroxidase (GSH-Px), hydrogen peroxide (H_2O_2), malondialdehyde, myeloperoxidase (MPO), and GSH assay kits were purchased from Nanjing Jiancheng Bioengineering Institute. A terminal deoxynucleotidyl transferase-mediated dUTP nick-end labeling (TUNEL) assay kit was obtained from Beyotime Biotechnology. A total RNA extraction kit was purchased from Aidlab Biotechnologies. Primescript™ First-Strand cDNA Synthesis and RT-PCR kits were obtained from TaKaRa. Antibodies against cleaved caspase-3, phosphor-IκB (p-IκB), IκB, phosphor-P65 (p-P65), and P65 were products of Cell Signaling Technology. Antibodies against GAPDH, nuclear factor (erythroid-derived 2)-like 2 (NRF2), NAD(P)H dehydrogenase quinone 1 (NQO1), and B cell lymphoma 2-associated X protein (BAX) were procured from Santa Cruz Biotechnology. Purified anti-mouse F4/80 and CD11b were purchased from Biolegend, whereas purified anti-mouse Gr-1 was a product of BD Pharmingen. The Alexa Fluor® 594 AffiniPure Donkey Anti-Rat IgG was from Jackson ImmunoResearch Laboratories.

Experimental design

All experiments were approved by the Animal Care and Use Committee of China Agricultural University, and conformed to the Guide for the Care and Use of Laboratory Animals.

Experiment 1.

A total of 48 six-week-old male C57BL/6 mice with a body weight (BW) of 16 to 20 g (with a mean of 18 g; Huafukang Biotechnology Ltd) were housed in a room with a temperature of 22 to 24°C (with a mean of 23°C) and a 12-h light/12-h dark cycle. Mice had free access to feed (Huafukang Biotechnology Ltd, No. 1022) and drinking water. **Supplemental Table 1** presents the nutritional composition of the diet. Amino acid content in the basal diet was determined by HPLC as described previously (17), and **Supplemental Table 2** shows the results. Mice were randomly assigned into 1 of 4 groups ($n = 12$ per group): control (CON), Gly supplementation (GLY), LPS administration (LPS), and Gly + LPS coadministration (GLY + LPS). Mice received oral administration of water (CON) or Gly (5 g · kg BW^{-1} · d^{-1}) for 6 continuous days. On day 7, mice in the LPS group or the GLY + LPS group received intraperitoneal administration of LPS (5 mg/kg BW) to induce liver injury, whereas mice in the CON or GLY groups received intraperitoneal administration of an equal volume of PBS.

Experiment 2.

To determine the effect of Gly-driven GSH synthesis on the LPS-induced liver injury, 6-wk-old male C57BL/6 mice with a BW of 18 ± 2 g (mean ± SD) were randomly assigned to 1 of 4 groups ($n = 6$ per group): CON, LPS, GLY + LPS, and Gly + BSO + LPS coadministration (GLY + BSO + LPS). Mice were orally administered water (CON) or Gly (5 g · kg BW^{-1} · d^{-1}) for 6 continuous days in the presence or absence of BSO, an inhibitor of GSH synthesis (0.5 g/kg BW, intraperitoneally administered every other day during the 6-d-period). On the day 7, mice were intraperitoneally administrated with either LPS (5 mg/kg BW) to induce liver injury or an equal volume of PBS. The dose of Gly was based on our pilot study, whereas the doses of LPS and BSO were based on previous reports (18–21). **Supplemental Tables 3** and **4** summarize the intakes of feed, water, and Gly. Orbital blood was collected at 6 h after LPS injection. The right lobe of the liver was collected for histological or immunofluorescence analyses, as well as mRNA and protein extraction.

Histological analysis

Liver tissues fixed in 4% formaldehyde were dehydrated and embedded in paraffin, sectioned, and stained with hematoxylin and eosin. Sections from each mouse ($n = 6$) were visualized for the analysis of karyolysis and karyopyknosis by a blinded observer. The percentage of karyolysis or karyopyknosis was calculated by counting the number of positive cells in 100 cells in each of 5 randomly selected fields in each section. All sections were viewed at a magnification of 200 via a light microscope equipped with a computer-assisted morphometric system. Results were normalized to the CON group, and representative images are provided.

Biochemical index assay

Serum AST, ALT, and LDH activities were measured by using commercial kits according to the manufacturer's instructions (Nanjing).

Supported by National Natural Science Foundation of China grants 31572410, 31625025 (to ZW); "111" Project grant B16044; and Texas A&M AgriLife Research (H-8200).
Author disclosures: The authors report no conflicts of interest.
GW was a member of the *Journal*"s Editorial Board.
Supplemental Tables 1–5 and Supplemental Figures 1–3 are available from the "Supplementary data" link in the online posting of the article and from the same link in the online table of contents at https://academic.oup.com/jn/.
Address correspondence to ZW (e-mail: bio2046@hotmail.com).
Abbreviations used: ALT, alanine transaminase; AST, aspartate transaminase; BAX, B cell lymphoma 2-associated X protein; BSO, L-buthionine sulfoximine; BW, body weight; CAT, catalase; *Ccl*, chemokine (C-C motif) ligand; CON, control group; *Cox2*, cyclooxygenase 2; GLY + BSO + LPS, glycine + BSO + LPS coadministration group; GLY + LPS, glycine + LPS coadministration group; GSH, glutathione; GSH-Px, glutathione peroxidase; GSSG, oxidized glutathion; *Inos*, inducible nitric oxide synthase; LDH, lactate dehydrogenase; MPO, myeloperoxidase; NQO1, NAD(P)H dehydrogenase quinone 1; NRF2, nuclear factor (erythroid-derived 2)-like 2; p-IκB, phosphor-IκB; p-p65, phosphor-P65; ROS, reactive oxygen species; SOD, superoxide dismutase; T-GSH, total glutathione; TUNEL, terminal deoxynucleotidyl transferase-mediated dUTP nick-end labeling.

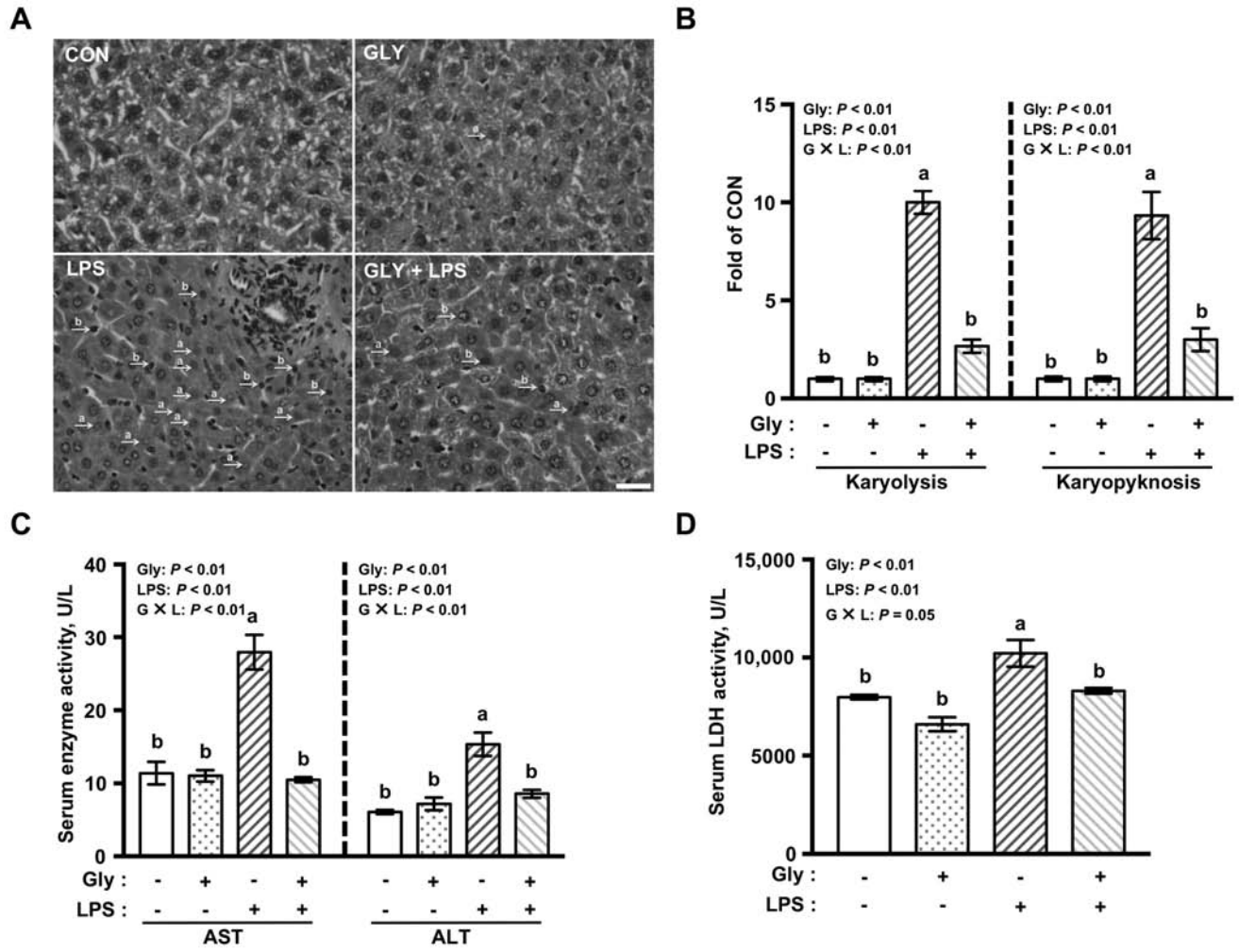

FIGURE 1 Liver histological alterations (A), the quantification of hepatic karyolysis and karyopyknosis (B), and serum AST, ALT, and LDH activities (C, D) in mice treated with water (CON), Gly, LPS, or Gly + LPS (Experiment 1). Data are means ± SEMs, $n = 6$. Means for an indicated parameter without a common letter differ, $P < 0.05$. (A) Arrow labels denote [a]karyolysis or [b]karyopyknosis. Scale bar, 25 μm. A color version of this figure is available as **Supplemental Figure 2**. ALT, alanine transaminase; AST, aspartate transaminase; CON, control group; G × L, Gly × LPS; GLY, glycine administration group; GLY + LPS, glycine plus LPS administration group; LDH, lactate dehydrogenase; LPS, LPS administration group.

Liver homogenates were used for the analyses of the malondialdehyde, MPO, H_2O_2, and GSH concentrations, and activities of antioxidative enzymes (SOD, CAT, and GSH-Px) by spectrophotometric methods, as instructed by the manufacturer (Nanjing). Data on hepatic GSH concentrations, malondialdehyde contents, as well as SOD, CAT, and GSH-Px activities are expressed per milligram of protein, whereas data on hepatic MPO activity and H_2O_2 concentration are expressed per gram of tissue or protein, respectively. All the optical density values were measured by using the SpectraMax M3® spectrophotometer (Molecular Devices).

TUNEL assay

Apoptotic assays were performed according to the manufacturer's instructions (Beyotime Biotech). Briefly, sections of the liver were permeabilized with 0.1% Triton X-100 for 2 min at room temperature, and then were incubated with a TUNEL reaction mixture for 1 h at 37°C. The nuclei were stained with Hoechst 33258 for 1 min at 25°C. Sections from each mouse ($n = 6$) in scrambled order were observed by a blinded observer under a fluorescence microscope (Axio Vert.A1, Zeiss). Apoptotic cells were quantified by randomly counting 5 different microscopic fields for each section. The percentage of apoptotic cells was calculated as the number of TUNEL-positive cells divided by the total number of cells, and is expressed as a fold change relative to the CON group.

Immunofluorescence

Inflammatory cell infiltration was assessed by immunofluorescence. Briefly, sections of the liver were blocked and then incubated with a primary antibody (F4/80, CD11b, or Gr-1) overnight at 4°C. After washing, sections were incubated with the Alexa Fluor 594-conjugated secondary antibody for 1 h at 25°C. Nuclei were stained by Hoechst 33258. Sections were visualized by a blinded observer using a fluorescence microscope (Axio Vert.A1, Zeiss). Immune cell infiltration was evaluated and is expressed as described for the TUNEL assay.

Real-time PCR

Total RNA was extracted and then reverse-transcribed into cDNA, as instructed by the manufacturer. Real-time PCR was performed using the SYBR Premix Ex Taq II (TaKaRa) and the ABI-Prism 7500 Sequence Detection System (Applied Biosystems) according to the manufacturers' instructions. **Supplemental Table 5** lists the primer sequences used in the present study. *Gapdh* was used as an internal control. The $2^{-\Delta\Delta CT}$ method was used to determine the fold change of the mRNA level.

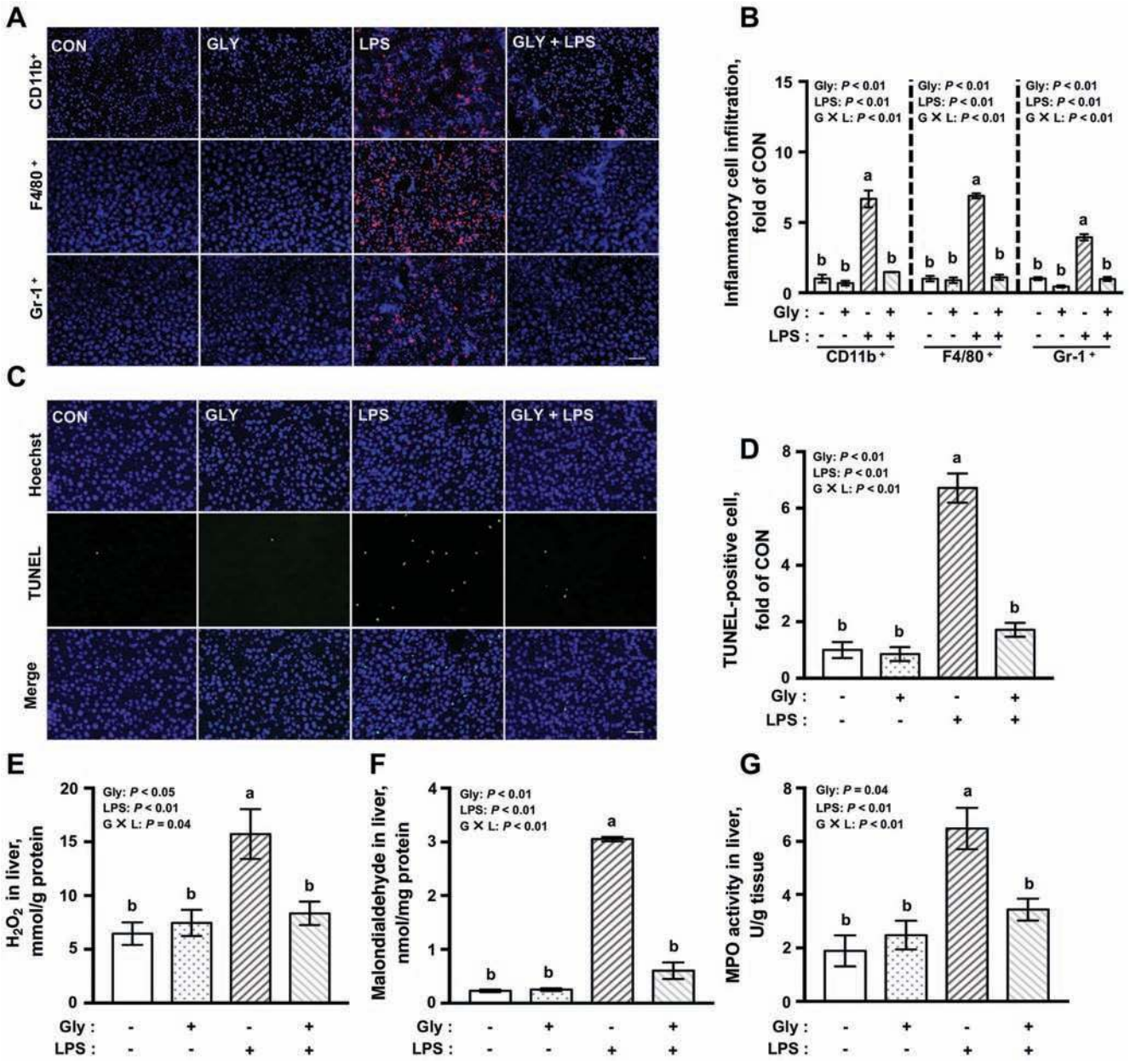

FIGURE 2 Immunofluorescence analysis (A) and quantification of immune cells in the liver (B), the TUNEL assay (C) and the quantification of TUNEL-positive cells in the liver (D), hepatic concentrations of H_2O_2 (E), and malondialdehyde (F), as well as hepatic MPO activity (G) in mice treated with water (CON), Gly, LPS, or Gly + LPS (Experiment 1). Data are means ± SEMs, $n = 6$. Means for an indicated parameter without a common letter differ, $P < 0.05$. The white bar in images is 20 μm. CON, control group; G × L, Gly × LPS; GLY, glycine administration group; GLY + LPS, glycine + LPS group; H_2O_2, hydrogen peroxide; LPS, LPS administration group; MPO, myeloperoxidase; TUNEL, terminal deoxynucleotidyl transferase-mediated dUTP nick end labeling.

Western blot

Liver samples were homogenized in liquid nitrogen for protein extraction. Protein abundance was determined by using the western blot technique, as described previously (22). The protein bands were developed by a chemiluminescence kit (Amersham Biosciences) using an Image Quant LAS 4000 mini system (GE Healthcare Bio-sciences). Protein band density was quantified by the Image software (GE Healthcare Life Sciences).

Statistical analysis

All data are presented as means ± SEMs and were analyzed by a normality test in SAS (SAS Institute Inc.). Results that followed the normal distribution were analyzed by 1- or 2-factor ANOVA in SAS. Results in Experiment 1 were analyzed by 2-factor ANOVA, whereas results in Experiment 2 were analyzed by 1-factor ANOVA. For 2-factor ANOVA, the PROC general linear model was used for the interaction test, with Gly and LPS as the main factors. Differences between means were determined by using the Student–Newman–Keuls multiple-comparison test. $P < 0.05$ was taken to indicate statistical significance.

Results

Gly supplementation ameliorated LPS-induced liver injury in mice

Compared with CON, LPS treatment led to morphological changes in the liver of mice, as shown by the presence of

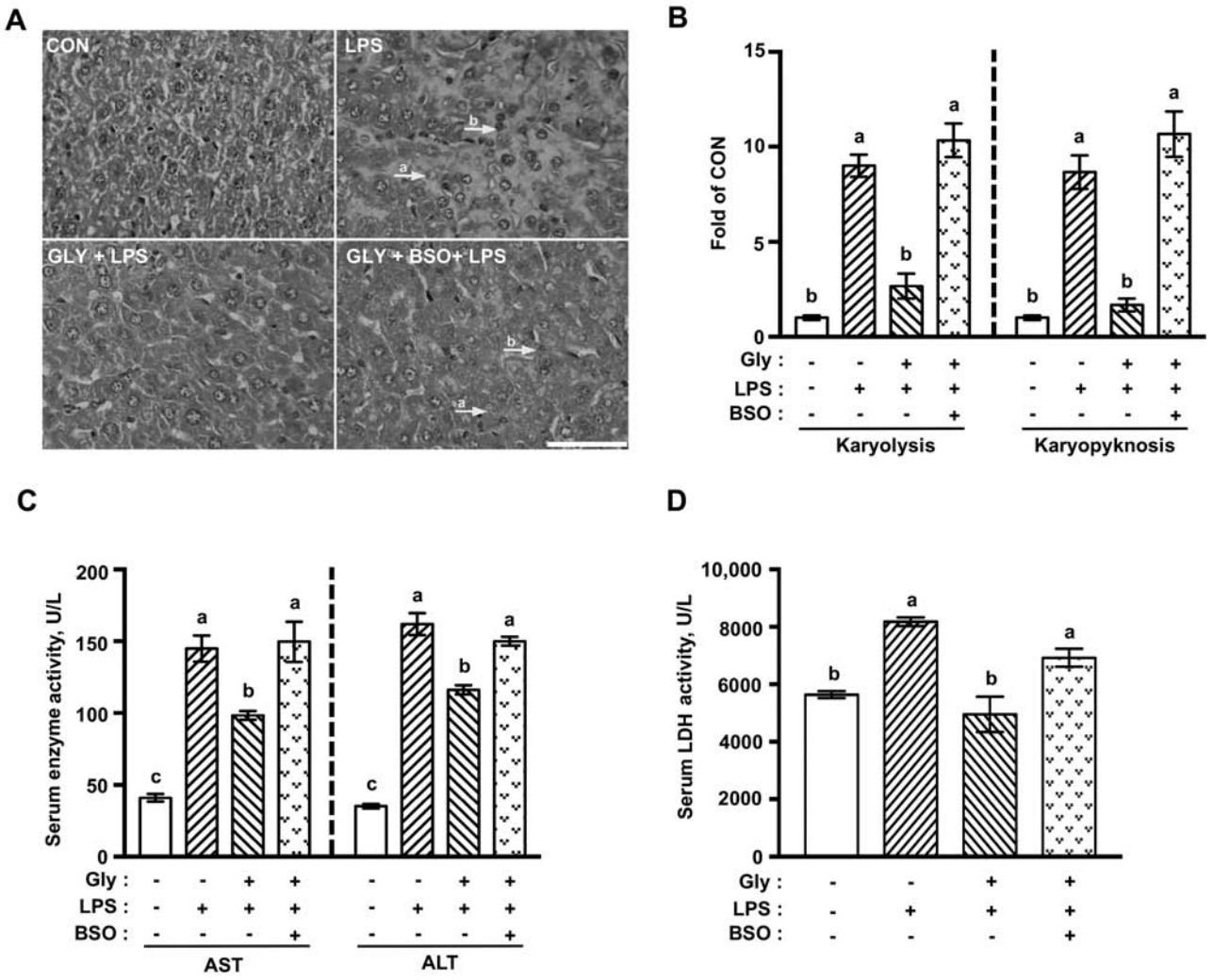

FIGURE 3 Liver hematoxylin and eosin staining (A), the quantification of hepatic karyolysis and karyopyknosis (B), and serum AST, ALT, and LDH activities (C, D) in mice treated with water (CON), LPS, Gly + LPS, or Gly + BSO + LPS (Experiment 2). Data are means ± SEMs, $n = 6$. Means for an indicated parameter without a common letter differ, $P < 0.05$. (A) Arrow labels denote [a]karyolysis or [b]karyopyknosis. Scale bar, 100 μm. A color version of this figure is available as **Supplemental Figure 3**. ALT, alanine transaminase; AST, aspartate transaminase; BSO, buthionine sulfoximine; CON, control group; GLY + BSO + LPS, glycine + BSO + LPS group; GLY + LPS, glycine + LPS group; LDH, lactate dehydrogenase; LPS, LPS administration group.

karyolysis and karyopyknosis (**Figure 1**A, B). These alterations were attenuated ($P < 0.05$) by Gly supplementation. Consistently, the activities of AST, ALT, and LDH in serum were enhanced ($P < 0.05$) by LPS, and these effects of LPS were abrogated by Gly supplementation (Figure 1C, D).

Gly supplementation attenuated inflammatory cell infiltration and apoptosis in the liver of LPS-challenged mice

Compared with CON, LPS treatment led to an increase in the infiltration of inflammatory cells, as the numbers of macrophages ($CD11b^+$, $F4/80^+$) and neutrophils ($Gr\text{-}1^+$) in the liver showed (**Figure 2**A, B). These adverse effects of LPS were reduced by Gly supplementation. Furthermore, LPS treatment increased the number of TUNEL-positive cells (Figure 2C, D), as compared with CON. Notably, Gly supplementation also ameliorated ($P < 0.05$) this effect of LPS . Biochemical analyses demonstrated that the concentrations of H_2O_2 and malondialdehyde, as well as MPO activity in the liver, were enhanced ($P < 0.05$) in LPS-challenged mice, as compared with CON, and Gly supplementation also ameliorated ($P < 0.05$) these adverse effects of LPS (Figure 2E-G).

GSH synthesis was required for a protective effect of Gly supplementation on liver injury

To elucidate the mechanisms responsible for the protective effect of Gly, mice were treated with vehicle buffer or BSO, an inhibitor of GSH synthesis. Histological analyses showed that the protective effects of Gly on LPS-induced morphological improvement were abolished ($P < 0.05$) by BSO (**Figure 3**A, B). Similar results were observed for the activities of AST, ALT, and LDH in the serum of mice (Figure 3C, D).

A protective effect of Gly on LPS-induced oxidative damage was dependent on GSH in the liver

To assess the role of GSH synthesis in the beneficial effect of Gly on hepatic oxidative damage, we determined the reduced form of glutathione (i.e., GSH), the oxidized form of glutathione (GSSG), and total GSH (T-GSH) in the liver. The results

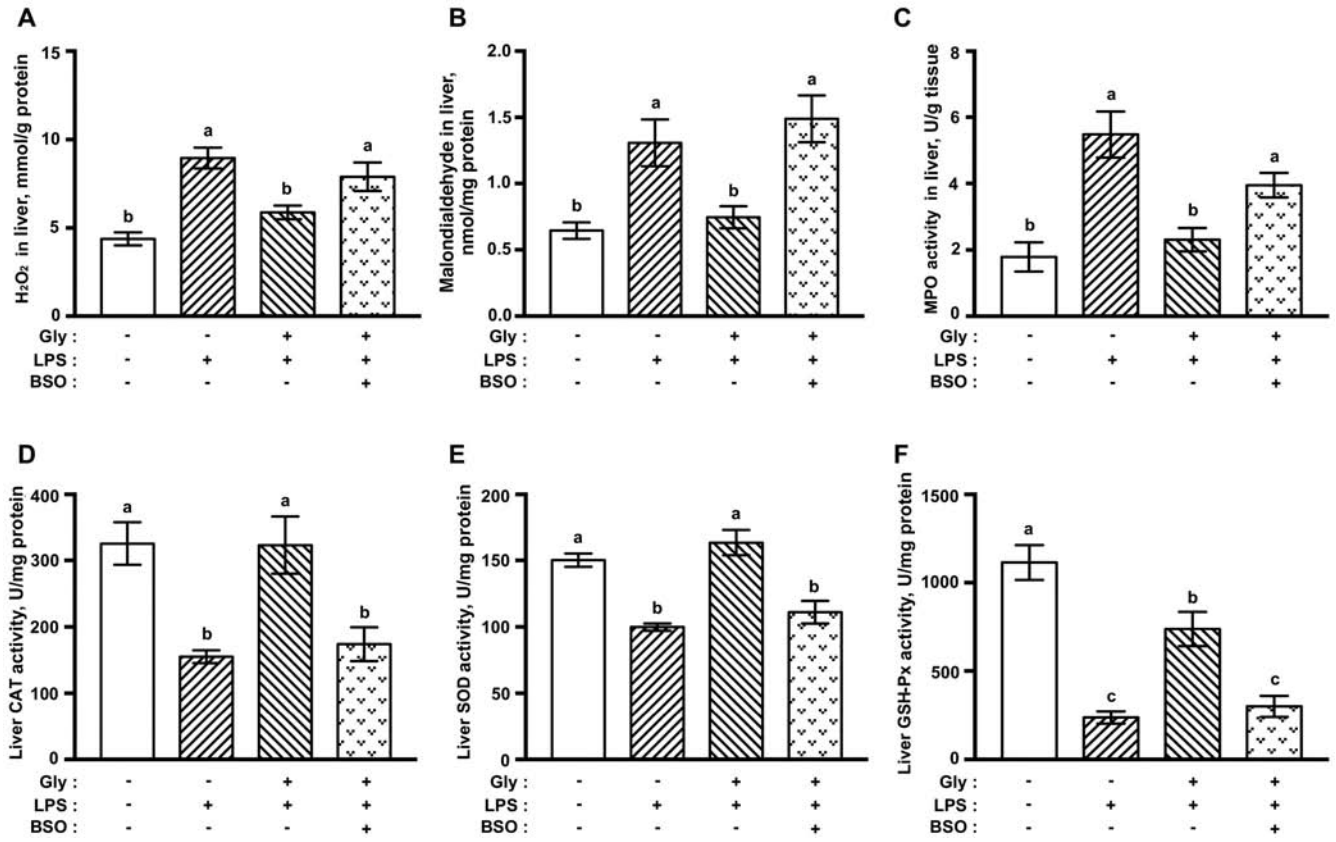

FIGURE 4 Concentrations of hepatic H_2O_2 (A) and malondialdehyde (B), as well as the hepatic activities of MPO (C), CAT (D), SOD (E), and GSH-Px (F) in mice treated with water (CON), LPS, Gly + LPS, or Gly + BSO + LPS (Experiment 2). Data are means ± SEMs, $n = 6$. Means without a common letter differ, $P < 0.05$. CAT, catalase; CON, control group; GLY + BSO + LPS, glycine + BSO + LPS group; GLY + LPS, glycine + LPS group; GSH-Px, glutathione peroxidase; H_2O_2, hydrogen peroxide; LPS, LPS group; MPO, myeloperoxidase; SOD, superoxide dismutase.

showed that LPS administration decreased ($P < 0.05$) hepatic GSH concentrations, and Gly supplementation prevented ($P < 0.05$) this adverse effect of LPS (**Supplemental Figure 1**A). Importantly, administration of BSO abolished ($P < 0.05$) the increase in hepatic GSH concentration brought about by Gly supplementation to LPS-challenged mice (Supplemental Figure 1A). In contrast, LPS alone or LPS + Gly cotreatment did not affect the hepatic concentrations of GSSG and T-GSH (Supplemental Figure 1B, C). Consistent with the data on intracellular concentration of GSH, the beneficial effects of Gly on the hepatic concentrations of H_2O_2 and malondialdehyde, as well as hepatic MPO activity, were abolished ($P < 0.05$) by in LPS-challenged mice (**Figure 4**A–C). We also determined the hepatic activities of the major antioxidative enzymes CAT, SOD, and GSH-Px. Results indicated that LPS administration decreased the activities of these enzymes, and Gly supplementation prevented these adverse effects of LPS. Likewise, BSO abolished ($P < 0.05$) these beneficial effects of Gly on the liver (Figure 4D–F).

GSH synthesis was required for Gly to attenuate inflammatory cell infiltration in the liver of LPS-challenged mice

The protective effect of Gly on the infiltration of inflammatory cells into the liver, as evidenced by the reduced numbers of macrophages ($CD11b^+$, $F4/80^+$) and neutrophils ($Gr\text{-}1^+$) in the liver of LPS-challenged mice, was abolished ($P < 0.05$) by BSO (**Figure 5**A, B). Real-time PCR analysis showed that LPS increased ($P < 0.05$) mRNA levels for proinflammatory cytokines, including *Tnfa*, *Il1b*, *Il6*, *cyclooxygenase 2* (*Cox2*), and *inducible nitric oxide synthase* (*Inos*), and Gly supplementation attenuated ($P < 0.05$) these effects of LPS (Figure 5C). Again, BSO abolished ($P < 0.05$) the beneficial effects of Gly. We also determined the mRNA levels for chemokines, including *chemokine (C-C motif) ligand* (*Ccl*) *1*, *2*, *3*, and *8*. Compared with CON, mice treated with LPS exhibited increases ($P < 0.05$) in the mRNA levels of *Ccl1*, *2*, *3*, and *8*, and Gly treatment prevented ($P < 0.05$) these adverse effects of LPS. The effects of Gly supplementation on the expression of *Ccl1*, *3*, and *8*, but not *Ccl2*, in the liver of LPS-treated mice, were prevented ($P < 0.05$) by BSO (Figure 5D).

NF-κB and NRF2 signaling pathways were involved in the protective effect of Gly supplementation on LPS-induced liver injury in mice

Western blot results showed that LPS increased the protein abundances of p-IκB and its downstream target p-P65, indicating the activation of NF-κB signaling. Gly supplementation prevented ($P < 0.05$) the LPS-induced activation of NF-κB in the liver. BSO abolished ($P < 0.05$) this beneficial effect of Gly (**Figure 6**A, B). In addition, LPS decreased ($P < 0.05$) the protein abundances of NRF2 (a transcriptional factor related to oxidative stress) and its downstream target NQO1, but Gly supplementation alleviated ($P < 0.05$) these adverse effects of LPS. Of note, BSO abrogated ($P < 0.05$) these beneficial effects of Gly on the liver (Figure 6C, D).

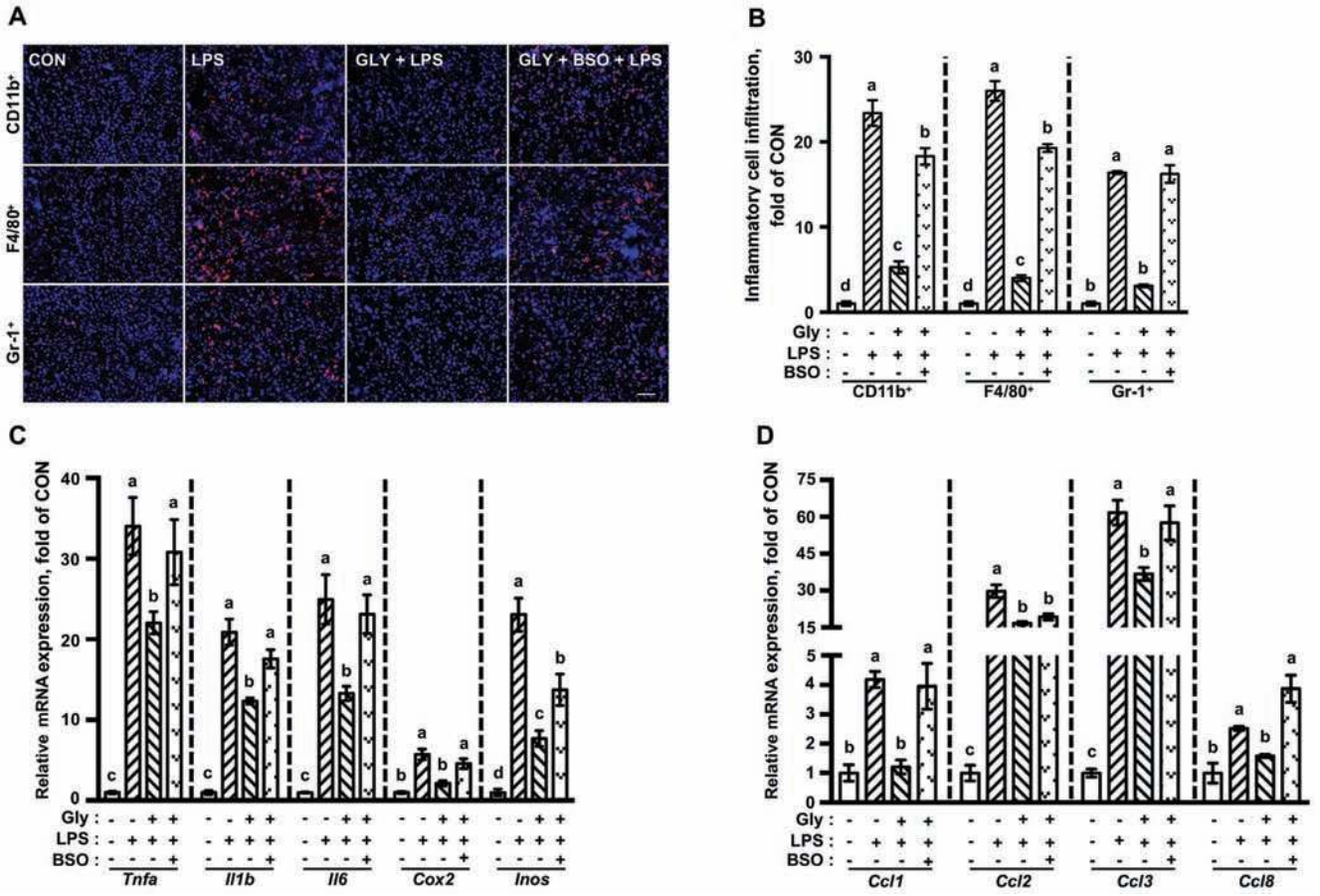

FIGURE 5 Immunofluorescence analysis (A) and quantification of immune cells (B) in the liver, as well as hepatic mRNA levels for proinflammatory cytokines (C) and chemokines (D) in mice treated with water (CON), LPS, Gly + LPS, or Gly + BSO + LPS (Experiment 2). *Gapdh* was used as a reference gene. Data are means ± SEMs, $n = 6$. Means without a common letter differ, $P < 0.05$. Scale bar, 20 μm. BSO, buthionine sulfoximine; *Ccl*, *chemokine (C-C motif) ligand*; CON, control group; *Cox2*, *cyclooxygenase 2*; GLY + BSO + LPS, glycine + BSO + LPS group; GLY + LPS, glycine + LPS group; *Il1b*, *IL-1β*; *Il6*, *IL-6*; *Inos*, *inducible nitric oxide synthase*; LPS, LPS group; *Tnfa*, *TNF-α*.

A protective effect of Gly on apoptosis in LPS-challenged mice was blocked by an inhibitor of GSH synthesis

Results of the TUNEL assay showed that Gly supplementation reduced ($P < 0.05$) the LPS-induced apoptosis in the liver (**Figure 7**A, B). The protective effect of Gly was dependent on GSH synthesis because the antiapoptosis effect of Gly was not observed in the presence of BSO (Figure 7A, B). In agreement with these observations, LPS treatment led to enhanced protein concentrations for cleaved caspase-3 and BAX ($P < 0.05$), but Gly largely abolished ($P < 0.05$) these adverse effects of LPS. Again, BSO abrogated ($P < 0.05$) the beneficial effects of Gly on cleaved caspase-3 and BAX expression (Figure 7C, D).

Discussion

Dysfunction of the liver is a global health problem owing to its multiple physiological roles in detoxification and metabolic homeostasis. In the present study, mice unsupplemented or supplemented with Gly received intraperitoneal administration of LPS, which has been reported to induce acute liver injury (18, 19). Consistently with previous studies (23, 24), LPS resulted in hepatic injury as shown by histological alterations of the liver and the enhanced activities of AST, ALT, and LDH in serum. In addition, we observed increases in the concentrations of H_2O_2 and malondialdehyde, MPO activity, apoptosis, and inflammatory response in the liver of LPS-challenged mice. Hepatic activities of SOD, CAT, and GSH-Px, which are antioxidative enzymes responsible for the elimination of free oxygen radicals (25), were reduced in response to LPS. Thus, the LPS administration reduced antioxidative enzymes, leading to the accumulation of ROS in the liver, which, in turn, resulted in enhanced concentrations of H_2O_2 and malondialdehyde. Of note, the deleterious effects of LPS on hepatic oxidative damage as indicated by histological alterations, as well as the enhanced protein concentrations of cleaved caspase-3 and BAX (2 proapoptotic proteins), were attenuated by Gly supplementation, suggesting a protective effect of Gly on liver injury in mice.

Gly is a substrate for the synthesis of GSH, an endogenous antioxidant required for the maintenance of intracellular homeostasis (12). GSH has been reported to protect the liver against oxidative stress (indicated by a decrease in the hepatic concentration of malondialdehyde) by augmenting the hepatic activities of CAT and SOD (26, 27). To investigate a functional role of GSH synthesis in alleviating the LPS-induced liver injury, mice receiving LPS administration were treated with vehicle solution or BSO, an inhibitor of GSH synthesis (16). Consistent with changes in the intracellular concentration of GSH, the beneficial effects of Gly on liver morphology; activities of AST, ALT, and LDH in serum; hepatic concentrations of H_2O_2 and

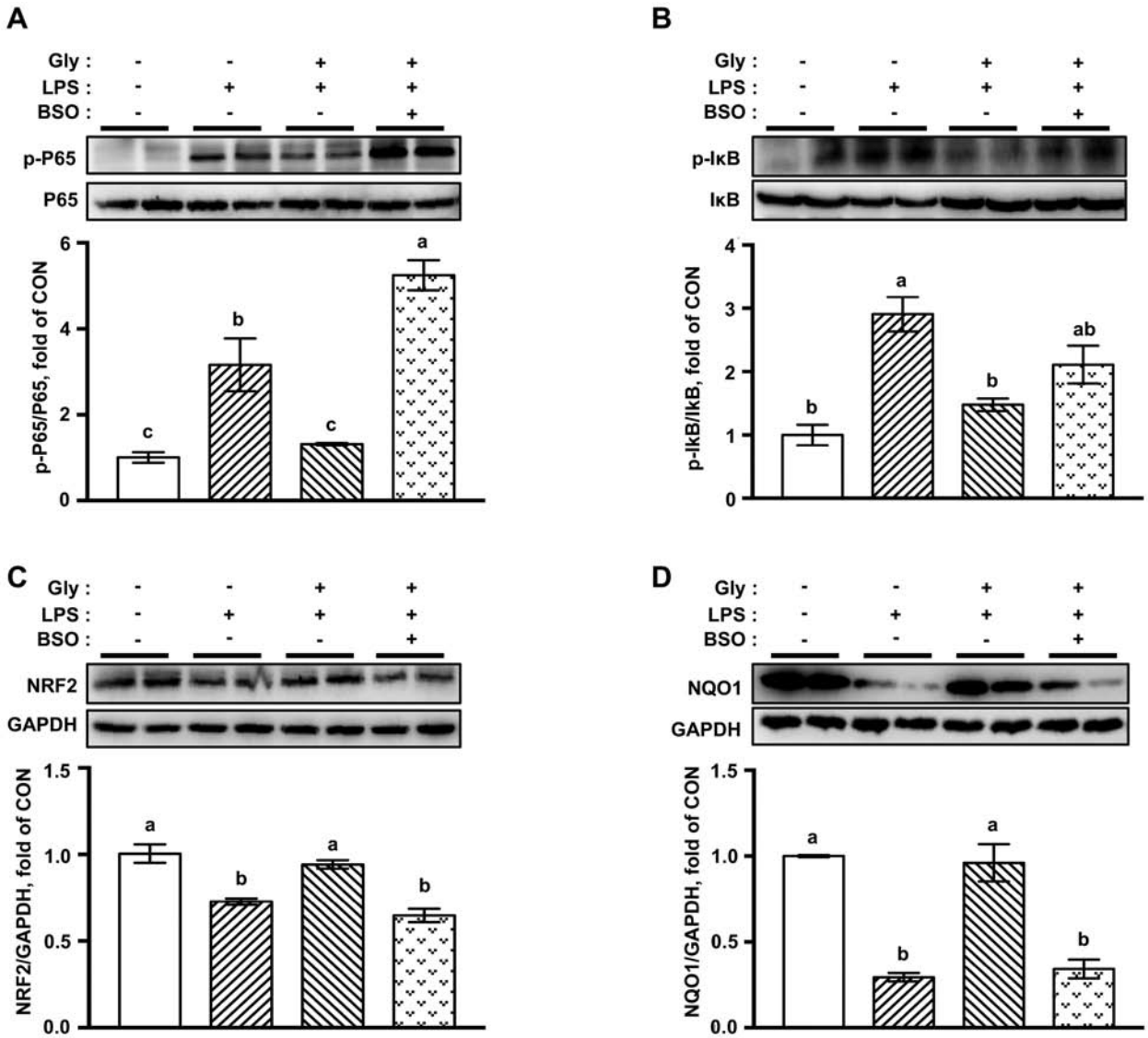

FIGURE 6 Western blot analysis of protein abundances for p-P65 (A), p-IκB (B), NRF2 (C), and NQO1 (D) in the liver of mice treated with water (CON), LPS, Gly + LPS, or Gly + BSO + LPS (Experiment 2). GAPDH was used as a loading control. Data are means ± SEMs, $n = 6$. Means without a common letter differ, $P < 0.05$. BSO, buthionine sulfoximine; CON, control group; GLY + BSO + LPS, glycine + BSO + LPS group; GLY + LPS, glycine + LPS group; LPS, LPS group; NQO1, NAD(P)H dehydrogenase quinone 1; NRF2, nuclear factor (erythroid-derived 2)-like 2; p-IκB, phospho-IκB; p-P65, phospho-P65.

malondialdehyde; and hepatic MPO activity in LPS-challenged mice were abrogated by BSO. Similar results were observed for the activities of antioxidative enzymes (CAT, SOD, and GSH-Px) and apoptosis in the liver. All these findings indicated an important role of Gly in protecting the liver from LPS-induced injury through the GSH-dependent antioxidant system.

Excessive ROS has been reported to activate immune responses and contribute to the pathogenesis of liver diseases (28–30). In the present study, we observed an increase in the activity of MPO, a member of the heme peroxidase superfamily proteins produced by monocytes, neutrophils, and macrophages (31), in the liver of LPS-challenged mice, indicating the activation of immune responses in our mouse model. Using specific antibodies against biomarker proteins related to immune cells, we found that LPS induced the infiltration of $CD11b^+$, $F4/80^+$ macrophages, and $Gr\text{-}1^+$ neutrophils into the liver, while increasing the hepatic mRNA levels for inflammatory cytokines (*Tnfa*, *Il1b*, *Il6*, *Cox2*, *Inos*, and *Ccl1*, *2*, *3*, and *8*). These results are in agreement with those from a previous study (32). Notably, Gly supplementation prevented the activation of immune cells and BSO abolished this effect of Gly, further supporting a critical role for GSH restoration in ameliorating the LPS-induced liver injury.

NF-κB, the central regulator of inflammatory cytokines, plays an important role in the development of hepatocellular injury, liver fibrosis, and hepatocellular carcinoma (33). LPS has been reported to activate the NF-κB signal pathway as well as the production of its downstream proinflammatory cytokines and chemokines owing to ROS accumulation (34, 35). Interestingly, Gly supplementation inactivated IκB, an upstream regulator of the NF-κB signaling, thus blocking NF-κB activity and attenuating the actions of inflammatory cytokines and chemokines. The regulatory effect of Gly was mediated by GSH synthesis, as noted previously. It is unknown how Gly inhibits the expression of NF-κB, but it is possible that the underlying mechanisms may involve cellular antioxidative signaling. More

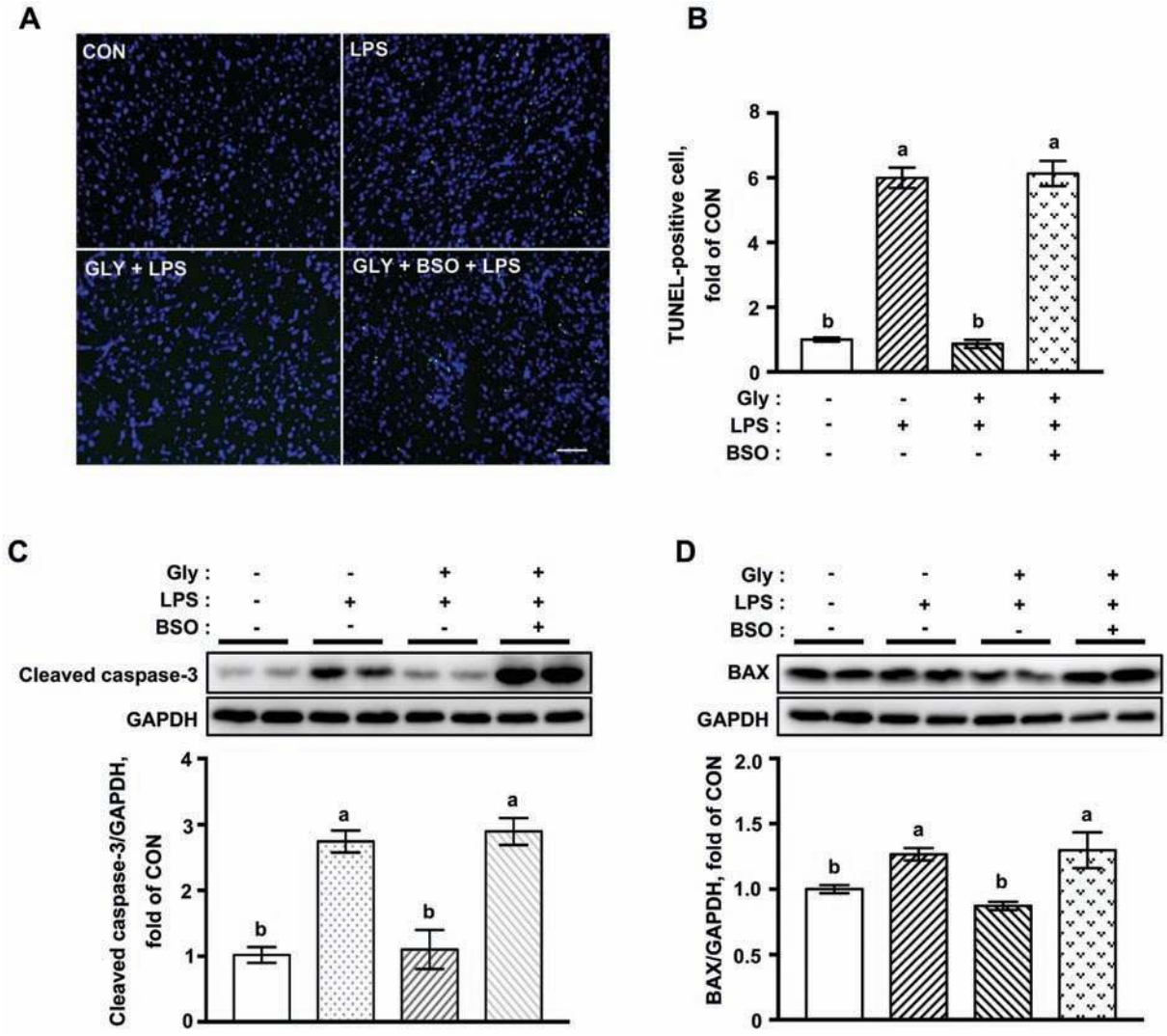

FIGURE 7 TUNEL assay (A) and quantification of TUNEL-positive cells (B) in the liver, as well as western blot analysis of hepatic protein abundances for cleaved caspase-3 (C) and BAX (D) in mice treated with water (CON), LPS, Gly + LPS, or Gly + BSO + LPS (Experiment 2). GAPDH was used as a loading control. Data are means ± SEMs, $n = 6$. Means without a common letter differ, $P < 0.05$. Scale bar, 20 μm. BAX, B cell lymphoma 2-associated X protein; BSO, buthionine sulfoximine; CON, control group; GLY + BSO + LPS, glycine + BSO + LPS group; GLY + LPS, glycine + LPS group; LPS, LPS group; TUNEL, terminal deoxynucleotidyl transferase-mediated dUTP nick-end labeling.

studies are required to investigate whether redox or calcium signaling results in the beneficial effect of Gly in the liver, as suggested for other organs (36). In addition, several lines of studies indicated that NRF2 can regulate the expression of enzymes involved in GSH biosynthesis, thus protecting cells from oxidative stress–induced cellular damage and apoptosis by reducing ROS (37, 38). In the present study, the protein concentrations of NRF2 and its downstream target NQO1 were reduced by LPS administration in the mouse liver. Of particular note, Gly supplementation abrogated this effect of LPS when hepatic GSH synthesis was not inhibited, implicating a key regulatory role of Gly in NRF2 signaling. This mechanism, together with the NF-κB signaling, may help to explain the protective role of Gly as a functional amino acid (39) in the liver of LPS-treated mice.

In conclusion, Gly administration ameliorated LPS-induced apoptosis, reduced the infiltration of inflammatory cells, and attenuated the elevated concentrations of inflammatory cytokines and chemokines in the liver of mice by enhancing hepatic GSH synthesis. This effect of Gly was associated with the inhibition of NF-κB and the activation of the NRF2 signaling pathway. Our findings provide new evidence that dietary Gly supplementation is a nutritional strategy to alleviate endotoxin-induced liver damage in mice.

Acknowledgments

The authors' responsibilities were as follows—YZ and ZW: designed the study, conducted the experiment, and wrote the manuscript; HJ, CW, and YJ: assisted with the experiment; NL and JC: assisted with technical skills in the experiment; YY, ZW, and GW: edited the manuscript; ZD and GW: analyzed the data; ZW and GW: had primary responsibility for the final content; and all authors: read and approved the final manuscript.

References

1. Robinson MW, Harmon C, O'Farrelly C. Liver immunology and its role in inflammation and homeostasis. Cell Mol Immunol 2016;13:267–76.
2. Wang D, Gao Q, Zhao G, Kan Z, Wang X, Wang H, Huang J, Wang T, Qian F, Ho CT, et al. Protective effect and mechanism of theanine on lipopolysaccharide-induced inflammation and acute liver injury in mice. J Agric Food Chem 2018;66:7674–83.

3. Fang YZ, Yang S, Wu G. Free radicals, antioxidants, and nutrition. Nutrition 2002;18:872–9.
4. Schieber M, Chandel NS. ROS function in redox signaling and oxidative stress. Curr Biol 2014;24:R453–62.
5. Kumar V, Sharma M, Lemos M, Shriram V. Efficacy of *Helicteres isora* L. against free radicals, lipid peroxidation, protein oxidation and DNA damage. J Pharm Res 2013;6:620–5.
6. Liu T, Zhang L, Joo D, Sun SC. NF-κB signaling in inflammation. Sig Transduct Target Ther 2017;2:17023.
7. Fornari F, Pollutri D, Patrizi C, La Bella T, Marinelli S, Casadei Gardini A, Marisi G, Baron Toaldo M, Baglioni M, Salvatore V, et al. In hepatocellular carcinoma miR-221 modulates sorafenib resistance through inhibition of caspase-3-mediated apoptosis. Clin Cancer Res 2017;23:3953–65.
8. Wang K. Molecular mechanisms of hepatic apoptosis. Cell Death Dis 2014;5:e996.
9. Wang W, Wu Z, Dai Z, Yang Y, Wang J, Wu G. Glycine metabolism in animals and humans: implications for nutrition and health. Amino Acids 2013;45:463–77.
10. Razak MA, Begum PS, Viswanath B, Rajagopal S. Multifarious beneficial effect of nonessential amino acid, glycine: a review. Oxid Med Cell Longev 2017:1716701.
11. Ham DJ, Caldow MK, Chhen V, Chee A, Wang X, Proud CG, Lynch GS, Koopman R. Glycine restores the anabolic response to leucine in a mouse model of acute inflammation. Am J Physiol Endocrinol Metab 2016;310:E970–81.
12. McCarty MF, O'Keefe JH, DiNicolantonio JJ. Dietary glycine is rate-limiting for glutathione synthesis and may have broad potential for health protection. Ochsner J 2018;18:81–7.
13. Sun K, Wu Z, Ji Y, Wu G. Glycine regulates protein turnover by activating protein kinase B/mammalian target of rapamycin and by inhibiting *MuRF1* and *Atrogin-1* gene expression in C2C12 myoblasts. J Nutr 2016;146:2461–7.
14. Li W, Sun K, Ji Y, Wu Z, Wang W, Dai Z, Wu G. Glycine regulates expression and distribution of claudin-7 and ZO-3 proteins in intestinal porcine epithelial cells. J Nutr 2016;146:964–9.
15. Wang W, Wu Z, Lin G, Hu S, Wang B, Dai Z, Wu G. Glycine stimulates protein synthesis and inhibits oxidative stress in pig small intestinal epithelial cells. J Nutr 2014;144:1540–8.
16. Haddad JJ. L-buthionine-(S,R)-sulfoximine, an irreversible inhibitor of gamma-glutamylcysteine synthetase, augments LPS-mediated pro-inflammatory cytokine biosynthesis: evidence for the implication of an IkappaB-alpha/NF-kappaB insensitive pathway. Eur Cytokine Netw 2001;12:614–24.
17. Wu G, Meininger CJ. Analysis of citrulline, arginine, and methylarginines using high-performance liquid chromatography. Methods Enzymol 2008;440:177–89.
18. Huh Y, Keep RF, Smith DE. Impact of lipopolysaccharide-induced inflammation on the disposition of the aminocephalosporin cefadroxil. Antimicrob Agents Chemother 2013;57:6171–8.
19. Hwang JS, Kim KH, Park J, Kim SM, Cho H, Lee Y, Han IO. Glucosamine improves survival in a mouse model of sepsis and attenuates sepsis-induced lung injury and inflammation. J Biol Chem 2019;294:608–22.
20. Drew R, Miners JO. The effects of buthionine sulphoximine (BSO) on glutathione depletion and xenobiotic biotransformation. Biochem Pharmacol 1984;33:2989–94.
21. Revesz L, Edgren MR, Wainson AA. Selective toxicity of buthionine sulfoximine (BSO) to melanoma cells *in vitro* and *in vivo*. Int J Radiat Oncol Biol Phys 1994;29:403–6.
22. Wang H, Zhang C, Wu G, Sun Y, Wang B, He B, Dai Z, Wu Z. Glutamine enhances tight junction protein expression and modulates corticotropin-releasing factor signaling in the jejunum of weanling piglets. J Nutr 2015;145:25–31.
23. Jiang Z, Meng Y, Bo L, Wang C, Bian J, Deng X. Sophocarpine attenuates LPS-induced liver injury and improves survival of mice through suppressing oxidative stress, inflammation, and apoptosis. Mediators Inflamm 2018:5871431.
24. Yang YQ, Yan XT, Wang K, Tian RM, Lu ZY, Wu LL, Xu HT, Wu YS, Liu XS, Mao W, et al. Triptriolide alleviates lipopolysaccharide-induced liver injury by NRF2 and NF-κB signaling pathways. Front Pharmacol 2018;9:999.
25. Birben E, Sahiner UM, Sackesen C, Erzurum S, Kalayci O. Oxidative stress and antioxidant defense. World Allergy Organ J 2012;5:9–19.
26. Lin Y, Li Y, Hu X, Liu Z, Chen J, Lu Y, Liu J, Liao S, Zhang Y, Liang R, et al. The hepatoprotective role of reduced glutathione and its underlying mechanism in oxaliplatin-induced acute liver injury. Oncol Lett 2018;15:2266–72.
27. Wang J, Chen Y, Gao N, Wang Y, Tian Y, Wu J, Zhang J, Zhu J, Fan D, An J. Inhibitory effect of glutathione on oxidative liver injury induced by dengue virus serotype 2 infections in mice. PLoS One 2013;8:e55407.
28. Kolac UK, Ustuner MC, Tekin N, Ustuner D, Colak E, Entok E. The anti-inflammatory and antioxidant effects of *Salvia officinalis* on lipopolysaccharide-induced inflammation in rats. J Med Food 2017;20:1193–200.
29. Jung JY, Park SM, Ko HL, Lee JR, Park CA, Byun SH, Ku SK, Cho IJ, Kim SC. *Epimedium koreanum* ameliorates oxidative stress-mediated liver injury by activating nuclear factor erythroid 2-related factor 2. Am J Chin Med 2018;46:469–88.
30. Reyes-Gordillo K, Shah R, Muriel P. Oxidative stress and inflammation in hepatic diseases: current and future therapy. Oxid Med Cell Longev 2017:3140673.
31. Shaeib F, Khan SN, Thakur M, Kohan-Ghadr H-R, Drewlo S, Saed GM, Pennathur S, Abu-Soud HM. The impact of myeloperoxidase and activated macrophages on metaphase II mouse oocyte quality. PLoS One 2016;11:e0151160.
32. Karlmark KR, Wasmuth HE, Trautwein C, Tacke F. Chemokine-directed immune cell infiltration in acute and chronic liver disease. Expert Rev Gastroenterol Hepatol 2008;2:233–42.
33. Luedde T, Schwabe RF. NF-κB in the liver—linking injury, fibrosis and hepatocellular carcinoma. Nat Rev Gastroenterol Hepatol 2011;8:108–18.
34. Narayanan A, Amaya M, Voss K, Chung M, Benedict A, Sampey G, Kehn-Hall K, Luchini A, Liotta L, Bailey C, et al. Reactive oxygen species activate NFκB (p65) and p53 and induce apoptosis in RVFV infected liver cells. Virology 2014;449:270–86.
35. El Kamouni S, El Kebbaj R, Andreoletti P, El Ktaibi A, Rharrassi I, Essamadi A, El Kebbaj MS, Mandard S, Latruffe N, Vamecq J, et al. Protective effect of argan and olive oils against LPS-induced oxidative stress and inflammation in mice livers. Int J Mol Sci 2017;18(10):2181.
36. Van den Eynden J, Ali SS, Horwood N, Carmans S, Brone B, Hellings N, Steels P, Harvey RJ, Rigo JM. Glycine and glycine receptor signalling in non-neuronal cells. Front Mol Neurosci 2009;2:9.
37. Kobayashi EH, Suzuki T, Funayama R, Nagashima T, Hayashi M, Sekine H, Tanaka N, Moriguchi T, Motohashi H, Nakayama K, et al. Nrf2 suppresses macrophage inflammatory response by blocking proinflammatory cytokine transcription. Nat Commun 2016;7:11624.
38. Zou X, Feng Z, Li Y, Wang Y, Wertz K, Weber P, Fu Y, Liu J. Stimulation of GSH synthesis to prevent oxidative stress-induced apoptosis by hydroxytyrosol in human retinal pigment epithelial cells: activation of NRF2 and JNK-p62/SQSTM1 pathways. J Nutr Biochem 2012;23:994–1006.
39. Wu G. Functional amino acids in growth, reproduction and health. Adv Nutr 2010;1:31–7.